JMEPEG (2015) 24:3982–3988
DOI: 10.1007/s11665-015-1663-2

1059-9495/$19.00

Initial Oxidation Behavior in Air of TiAl-2Nb and TiAl-8Nb Alloys Produced by Electron Beam Melting

M. Terner, S. Biamino, G. Baudana, A. Penna, P. Fino, M. Pavese, D. Ugues, and C. Badini

(Submitted March 13, 2015; in revised form June 22, 2015; published online August 20, 2015)

Titanium aluminide alloys are good candidates for structural applications thanks to their low density and good balance of properties up to relatively high temperatures. However, their application is still limited by significant oxidation. Four γ-TiAl alloys with different content of aluminum and niobium were produced by electron beam melting: Ti-45Al-2Cr-2Nb, Ti-48Al-2Cr-2Nb, Ti-45Al-2Cr-8Nb, and Ti-46Al-2Cr-8Nb. The behavior of these alloys in response to oxidation in air during constant heating up to 1000 °C and isothermal oxidation for 10 h at 850 and 950 °C were studied by thermogravimetric analysis. The mass gain due to oxidation of the low Nb-containing alloys was always at least twice that of the high Nb-containing alloys. Both low and high Nb-containing alloys exhibited on their surface oxidation products of the same nature: oxides TiO_2 and Al_2O_3, and nitrides TiN and Ti_2AlN. Niobium addition up to 8 at.% did not suppress the growth of rutile and promote the formation of a protective alumina layer. However, it efficiently reduced the formation of rutile, mainly responsible for the mass gain due to oxidation of γ-TiAl alloys and with tendency to spallation.

Keywords additive manufacturing, aero-engine components, intermetallics, oxidation, thermal analysis, x-ray analysis

1. Introduction

Extensive research has been conducted for years on the oxidation behavior of γ-TiAl alloys (Ref 1-8). Thanks to a low density (~4 g/cm^3) and specific properties similar to that of Ni-based superalloys, γ-TiAl alloys are of particular interest for the production of rotating parts in gas turbine aero-engines and automotive turbochargers (Ref 1-5, 7, 9). Rotating parts such as turbine and compressor blades are primarily subjected to centrifugal forces due to high speed rotation. The reduction of the overall weight of such parts would lead to lower constraints on both the parts and the supporting disks. Despite attractive mechanical properties, TiAl alloys early exhibited significant drawbacks (Ref 2, 3, 9). In particular, low ductility and fracture toughness are often recorded which is a serious concern for structural use especially in the aeronautics industry. In addition, γ-TiAl alloys experience rather severe oxidation over 700 °C forming a non-protective mixed scale (Ref 1-7, 9).

M. Terner, Department of Applied Science and Technology, Politecnico di Torino, Corso Duca degli Abruzzi 24, 10129 Turin, Italy; and Department of Materials Science and Engineering, Changwon National University, 20 Changwondaehakro, Uichang-gu, Changwon-si, Gyeongsangnam-do 641-773, Republic of Korea; **S. Biamino, G. Baudana, P. Fino, M. Pavese, D. Ugues,** and **C. Badini**, Department of Applied Science and Technology, Politecnico di Torino, Corso Duca degli Abruzzi 24, 10129 Turin, Italy; and **A. Penna**, Avio SpA, Via I Maggio 56, Rivalta, 10040 Turin, Italy. Contact e-mail: mathieu@changwon.ac.kr.

The material's properties of γ-TiAl alloys are very sensitive to the chemical composition and the microstructure. While microstructure has little influence on the oxidation resistance (though Becker et al. (Ref 10) suggested that Al is preferentially oxidized in a two phase structure), the chemical composition (i.e., the nature and content of alloying elements) might be optimized to increase oxidation resistance and maintain a good balance of properties (Ref 1-7, 9). The poor oxidation resistance of γ-TiAl alloys is attributed to the lack of protective alumina scales and deleterious rapid growth of rutile (Ref 2-4, 6). On the one hand, the oxidation resistance of TiAl alloys can be increased by promoting the formation of protective alumina. The idea is to decrease oxygen diffusivity and solubility and to increase the aluminum diffusivity. Another approach is to impede the growth of detrimental rutile which is responsible for most of the mass gain of TiAl alloys due to oxidation (Ref 2-4). The addition of refractory elements such as Nb, Ta, Mo, W, Zr, or Hf was found effective. The beneficial effect of Nb was widely published (Ref 1-10). Nb atoms are located exclusively on Ti sites for the equilibrium phases present in Nb-containing γ-TiAl alloys (Ref 2, 4, 6, 9, 10). Since rutile grows mainly by oxygen diffusion through the oxide scales via a vacancy mechanism, the substitution of Ti by Nb with a higher valence is believed to decrease the oxygen vacancy concentration and therefore hinder rutile growth (Ref 2, 4, 6, 10).

The first generations of Nb-containing γ-TiAl alloys were limited to about 2 at.% Nb addition (Ref 5, 9, 11). However, with the increasing demand on higher operation temperatures, γ-TiAl-based alloys with higher amount up to 10 at.% of Nb are being developed (Ref 2, 4, 5, 7-9, 11). In the present paper, four TiAl alloys with different amounts of Al and Nb were fabricated by Electron Beam Melting. The initial oxidation behavior after short time in air of these alloys were investigated by thermogravimetric analysis (TGA) and compared. TGA is a common technique used to study the oxidation behavior of materials and several research that have focused on the oxidation behavior of TiAl alloys by this means (Ref 12-16).

2. Materials and Methods

2.1 Materials

Two low Nb-containing and two high Nb-containing γ-TiAl alloys were produced by Electron Beam Melting from gas atomized pre-alloyed powders. The complete description of the manufacturing process had been previously described by the authors (Ref 17). The actual chemical compositions of the massive materials after fabrication were measured by scanning electron microscopy (SEM-FEG Assing SUPRA 25) coupled with energy dispersive spectroscopy (EDS Oxford INCA x-Sight analyzer). Table 1 gives the chemical composition in at.% of the four alloys. For better convenience, the different alloys are identified in the following as TiAl45-2, TiAl48-2, TiAl45-8, and TiAl46-8 in correspondence with the Al and Nb content. The four alloys had different content of aluminum and niobium in order to highlight the role of the chemical composition on the oxidation behavior. The as-EBM microstructures of all four alloys were very similar and consisted in fully equiaxed α and γ grains. The high Nb-containing alloys exhibited a very low amount of β phase at grain boundaries which was considered having no significant effect on oxidation.

2.2 Thermogravimetry

Small $5 \times 5x5$ mm^3 cubic samples of each material were precisely cut from the core of as-EBM bars for TGA (Mettler Toledo AG—TGA/STDA851e). All TGA were realized in a 50 mL/min air flow. The machine recorded the sample's weight during the test thanks to a μg precision balance. Each specimen for TGA was contained in a 150-μL alumina crucible so that when spallation occurred, the weight of the spalled oxides was considered. A first set of samples was heated one by one from 25 to 750 °C with a heating rate of 10 °C/min, and then the heating rate was reduced down to 0.5 °C/min from 750 up to 1000 °C in order to reduce dynamic effects. Another two sets of samples were subjected to short time isothermal oxidation for 10 h at 850 and 950 °C, respectively (samples were heated at 10 °C/min up to the isotherm temperature). Considering the potential application of this kind of material, for structural materials such as low pressure gas turbine blades and turbocharger, 10 h can decidedly be considered a short time. The macroscopic aspect of the samples after oxidation was systematically observed.

2.3 Phase Analysis

The composition of the oxides scale formed after oxidation was analyzed for each material. X-ray diffraction analysis (Panalytical X'PERT PRO PW3040/60, Cu K_α radiation) was realized on the surface of the oxidized specimens. Attention was paid not to contaminate the surface prior to XRD measurements. After oxidation at 950 °C for 10 h, the low Nb-containing alloys TiAl45-2 and TiAl48-2 exhibited significant spallation of the outer oxide scale. Nevertheless, XRD analyses were realized on the samples surface not considering the spalled oxide's flakes. For the sake of comparison, all measures were set in percentage. That is, the peak of the highest intensity was set to 1 and the values of the measures were accordingly divided by the highest value.

Table 1 Chemical composition in at.% measured by EDS of low and high Nb-containing TiAl alloys

	Al	Nb	Cr	Ti
TiAl45-2	45.1	2.0	2.0	Bal.
TiAl48-2	47.6	2.0	1.5	Bal.
TiAl45-8	44.5	7.7	1.7	Bal.
TiAl46-8	45.4	7.9	1.8	Bal.

3. Results and Discussion

3.1 Thermogravimetric Analysis in 50 mL/min Air Flow During Slow Heating Between 750 and 1000 °C

Four TiAl alloys produced by electron beam melting were subjected to constant heating in 50 mL/min air flow from 25 to 750 °C at 10 °C/min and from 750 to 1000 °C the heating was decreased to 0.5 °C/min. It is well known that up to 750 °C, such Nb-containing TiAl alloys do not show signs of significant oxidation (Ref 5, 7). Figure 1 shows the mass gain in mg/cm^2 of the tested specimens during TGA.

Negligible mass gain was observed up to 750 °C which justified the reduction of the heating rate only between 750 and 1000 °C. Low and high Nb-containing alloys exhibited the same behavior up to slightly over 800 °C. From 800 to 1000 °C in Fig. 1, similar oxidation behaviors were observed over 800 °C for both low Nb-containing and high Nb-containing alloys, respectively, though low and high Nb-containing alloys behaved differently. This is consistent with the fact that the Nb content has the greatest influence on the oxidation behavior of γ-TiAl alloys in this composition range (Ref 5, 6). Between 800 and 850 °C, the low Nb-containing alloys TiAl45-2 and TiAl48-2 experienced suddenly higher oxidation rate, while the high Nb-containing TiAl45-8 and TiAl46-8 did not (Fig. 1). It appears from Fig. 1 that in the vicinity of 850 °C, higher content of Nb impeded the accelerated oxidation suffered by TiAl45-2 and TiAl48-2. After oxidation up to 1000 °C, the mass gain of the low Nb-containing alloys was much higher than that of the high Nb-containing alloys (Table 2). All four materials exhibited signs of spallation. The low Nb-containing alloys TiAl45-2 and TiAl48-2 showed substantial spallation and almost the entire

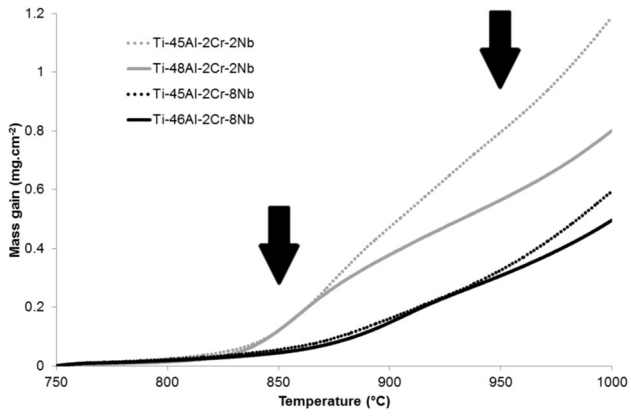

Fig. 1 Thermogravimetric analysis in 50 mL/min air flow of TiAl45-2, TiAl48-2, TiAl45-8, and TiAl46-8 during heating from 750 to 1000 °C at 0.5 °C/min

Table 2 Maximum weight gain in mg/cm^2 at the end of the oxidation experiments

	Constant heating to 1000 °C (0.5 °C/min)	Isothermal oxidation at 850 °C	Isothermal oxidation at 950 °C
TiAl45-2	1.189	0.615	1.202
TiAl48-2	0.801	0.437	0.805
TiAl45-8	0.595	0.184	0.399
TiAl46-8	0.496	0.186	0.412

external oxide layer had spalled. On the contrary, the high Nb-containing alloys TiAl45-8 and TiAl46-8 presented only minor spallation, mainly at corners and edges. From the TGA analysis under constant heating in Fig. 1, two temperatures stand out, 850 °C where the oxidation rate of low and high Nb-containing alloys start change significantly and 950 °C which is above the critical temperature for application of TiAl alloys (1, 4-7), respectively, pointed by black arrows. TiAl-based alloys with application temperatures as high as 950 °C would be of great benefit. On the one hand, it would largely overpass the maximum application temperature of lightweight Ti-based alloys (~700 °C). On the other hand, it would lead to a significant weight reduction replacing heavy Ni-based superalloys.

3.2 Thermogravimetric Analysis in 50 mL/min Air Flow for Short Time at 850 and 950 °C

The four γ-TiAl alloys were subjected to isothermal oxidation at 850 °C and at 950 °C for 10 h. In Fig. 2, the mass gain measured by TGA at 850 °C (Fig. 2a) and 950 °C (Fig. 2b) are plotted as a function of time for TiAl45-2, TiAl48-2, TiAl45-8, and TiAl46-8.

From Fig. 2, the high Nb-containing alloys TiAl45-8 and TiAl46-8 exhibited very similar behavior at both 850 and 950 °C. After a short transition or incubation time, the oxidation rates tended to stabilize quickly and the mass gain after 10 h were very low. On the contrary, the oxidation behaviors of the low Nb-containing alloys were substantially different from one another. At both 850 and 950 °C, the mass gain of TiAl45-2 due to oxidation was decidedly higher than that of TiAl48-2 (Fig. 2). In any case, the mass gain due to oxidation in air of the low Nb-containing alloys TiAl45-2 and TiAl48-2 were more than twice that of the high Nb-containing alloys TiAl45-8 and TiAl46-8 after 10 h in air at 850 and at 950 °C (Table 2). Moreover, the mass gain after 10 h at 850 °C of the low Nb-containing alloys was higher than that of the high Nb-containing alloys after 10 h at 950 °C (Table 2).

At 850 °C, the aspect of the oxides scale on the low Nb-containing alloys TiAl45-2 and TiAl48-2 was uniform, rather thick and with a light gray color. First signs of spallation could be seen on TiAl45-2. Instead, the aspect of the oxides scale on the high Nb-containing alloys TiAl45-8 and TiAl46-8 was thinner and had a dark blue shade. Moreover, the oxides scale was very consistent but somehow inhomogeneous and some lighter greenish areas were identified. At 950 °C, the oxidation clearly appeared more severe for both low and high Nb-containing alloys. Significant spallation was observed on both TiAl45-2 and TiAl48-2. Almost the entire external oxide layer had spalled for TiAl45-2 and only about half of the external layer remained consistent for TiAl48-2. The spalled oxides had

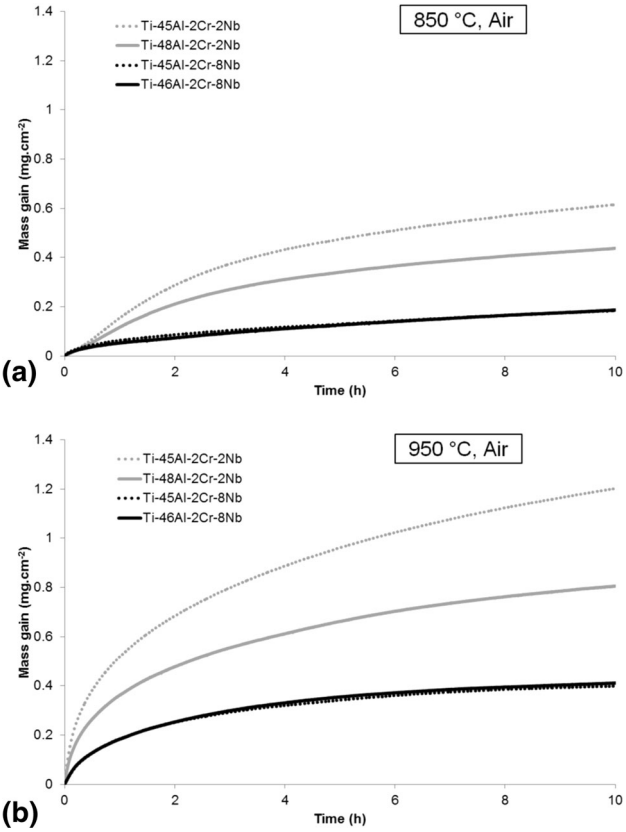

Fig. 2 Thermogravimetric analysis in 50 mL/min air flow of TiAl45-2, TiAl48-2, TiAl45-8, and TiAl46-8 during isothermal oxidation for 10 h at 850 °C (a) and 950 °C (b)

a light green/yellowish color, while the underlying oxides appeared like a mix of dark and light greenish color. TiAl45-8 and TiAl46-8 on the other hand exhibited oxides scales more consistent and had a gray color with some greenish areas. First signs of spallation were observed on TiAl46-8. Although it is hard to draw conclusions on this matter, the aspect of the oxide scales gave some information. After oxidation at 850 °C, the external oxide of the low Nb-containing alloys appeared much lighter than that on the high Nb-containing alloys which was dark. The external oxide scale is primarily composed of Titanium oxides when the Nb content is low (Ref 10). Therefore, it is appropriate to assume that the light gray color corresponds to oxides rich in Ti. The darker aspect of TiAl45-8 and TiAl46-8 after oxidation indicated that formation of TiO_2 was much lower than for TiAl45-2 and TiAl48-2. After oxidation at 950 °C, oxidation was more severe. The spalled external oxide layer, which was likely TiO_2 as confirmed by XRD and EDS, had a light green/yellowish color. This suggested that the formation of TiO2 oxide on high Nb-containing alloys was limited. It would certainly be of great interest to decidedly correlate the colors of the oxidation products as macroscopically observed with their nature.

From Fig. 2, it is clear that when the niobium content is low, here 2 at.%, the content of aluminum plays a role in the oxidation behavior of TiAl-2Nb alloys: the higher the Al content, the better the oxidation resistance (Ref 4, 6). A higher content of Al, and consequently a lower amount of Ti, promotes the formation of Aluminum oxides over Titanium oxides.

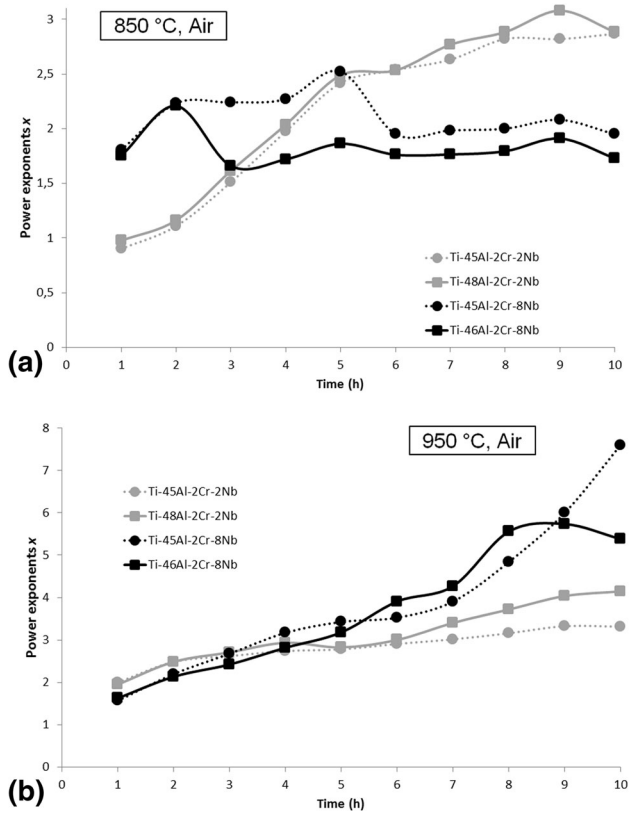

Fig. 3 Growth kinetic power exponent x from Eq **1** obtained from linear regression according to Eq **2** by 1-h step during isothermal oxidation in 50 mL/min air flow for 10 h at 850 °C (a) and 950 °C (b)

However, when the niobium content is high, here 8 at.%, the Al content in such range has very little influence on the oxidation resistance of TiAl-8Nb. Becker et al. (Ref 10) thoroughly studied the isothermal oxidation of TiAl alloys. The beneficial addition of Nb is acknowledged and is explained by promoting the formation of protective Al_2O_3. First, Nb stabilizes the γ-phase so that formation Al_2O_3 is promoted according to the Al-Ti-O phase diagram. Second, Nb addition decreases the activity ratio a_{Ti}/a_{Al} in the metal which favors the formation of protective Al_2O_3. Additionally, since Nb substitutes for Ti with a higher valence (5 and 4, respectively), several authors (Ref 2, 4) suggested that addition of such a dopant element decreases the oxygen vacancy concentration in the oxide and thus hinders the growth of TiO_2 mainly due to oxygen diffusion via a vacancy mechanism.The curves in Fig. 2 can be fitted by the following equation model (Ref 4, 8):

$$(\Delta M)^x = k_x t, \qquad \text{(Eq 1)}$$

where ΔM is the mass gain (here in mg/cm^2), x is the power exponent, k_x is the oxidation reaction rate constant (here in mg cm$^{x/2}$/h), and t is the oxidation time (here in h).

Equation (1) can be transformed into

$$x \cdot Ln(\Delta M) = Ln(k_x) + Ln(t). \qquad \text{(Eq 2)}$$

Subsequent linear regression of the curves $Ln(\Delta M) = f(Ln(t))$ allowed identify the values of the growth kinetic power exponents x for different periods of time. In order to investigate the kinetic behavior of the oxidation of the TiAl alloys, the values of the power exponent x (Eq 1) were determined by linear regression every 1-h step of the 10 h isothermal oxidation for each TiAl alloys. While Eq 1 typically describes the oxidation kinetics, it is hard to draw conclusions in the case of oxidation of TiAl which is defined by competitive oxidation of aluminum on one hand and titanium on the other hand. Therefore, from a chemical point of view, the kinetic power exponent x and the oxidation reaction rate constant k_x in Eq 1 are in reality a combination of x(Al), x(Ti) and k_x(Al), k_x(Ti) corresponding to the oxidation reaction of aluminum and titanium, respectively. In a two-product reaction with a common reactive, here oxygen reacts with Al and Ti, the reactions influence one another. Nevertheless, from a mathematical point of view, the equation model Eq 1 legitimately describes the oxidation kinetics, its evolution over time and the role of Nb content by comparison.

In Fig. 3, the values of the growth kinetic power exponents x (Eq 1) were plotted against time during 10 h oxidation in air at 850 °C (Fig. 3a) and 950 °C (Fig. 3b). The values reported at 1 h derive from the linear regression of the corresponding Eq 2 from the first hour of isothermal oxidation. Likewise, the values reported at 6 h in Fig. 3 derive from the linear regression from the sixth hour, i.e. between 5 and 6 h. Therefore, the graphs in Fig. 3 show the progress of the oxidation kinetics for all the alloys during isothermal oxidation.

Generally speaking, it can be noticed in Fig. 3 that the variations of the power exponent, which describes the oxidation kinetics behavior of the γ-TiAl alloys under investigation, was similar when the Nb content was similar. TiAl45-2 and TiAl48-2 exhibited similar values of x, so did TiAl45-8 and TiAl46-8. However, significant difference could be observed when the Nb content varied from 2 to 8 at.%. This confirmed the important role played by Nb addition on the oxidation behavior of γ-TiAl alloys. Note that the higher the power exponent x, the more "protective" the oxides scale.

In light gray in Fig. 3(a), the power exponents x (Eq. 1) increased similarly for the low Nb-containing alloys TiAl45-2 and TiAl48-2, from 1 to approximately 3 over the 10 h isothermal oxidation at 850 °C. This suggests that the initial oxides scale formed on these alloys were not protective, leading to a rather fast oxidation rate responsible for the initial higher mass gain experienced by low Nb-containing alloys (Fig. 2a). Over time, the oxidation rate decreased with the formation of protective aluminum oxides. Nevertheless, a substantial amount of titanium oxides, detrimental for oxidation resistance of such alloys, was formed. This assumption is supported by the higher mass gain experienced by the low Nb-containing alloys (Fig. 2a), titanium oxides being responsible for most of the mass gain of TiAl alloys due to oxidation (2-4). As mentioned earlier, oxidation of TiAl alloys is characterized by competitive oxidation of titanium and aluminum oxides. Becker et al. (Ref 10) discussed that Al_2O_3 precipitated may dissolve in TiO_2, which suggest that even though the power exponent increased up to about $x = 3$ for the low Nb-containing alloys, which suggest a lower oxidation rate at the time, the Al_2O_3 formed may be very unstable and may not have a protective behavior. In fact, peer studies have revealed that higher Nb content is beneficial during oxidation for longer time (Ref 2-8, 10, 14). The decrease of the oxidation rate (or increase of the power exponent) may arise from the formation of unstable Al_2O_3 with lower density compared to TiO_2.

On the other hand, in black in Fig. 3(a), the power exponents x (Eq 1) for the high Nb-containing alloys TiAl45-

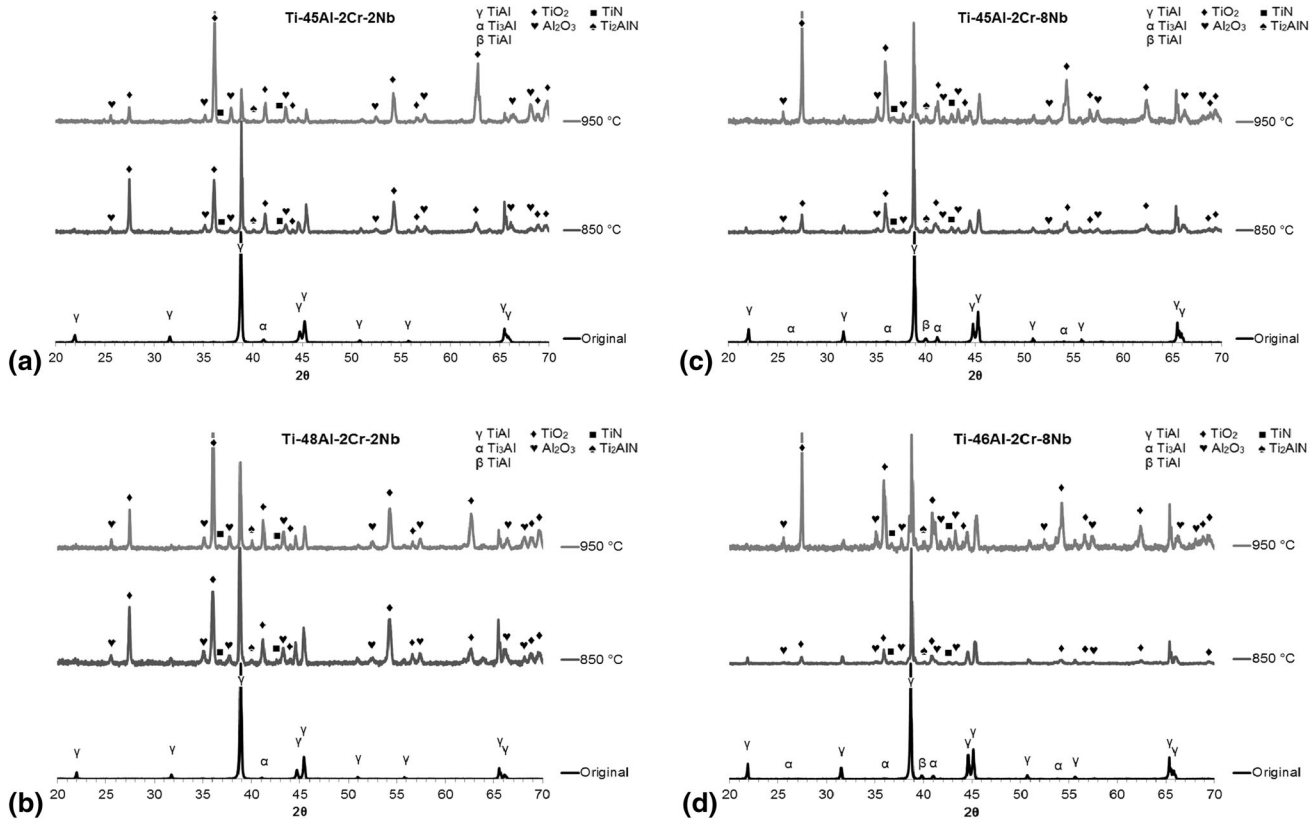

Fig. 4 X-ray diffraction patterns of the oxidized surface of TiAl45-2 (a), TiAl48-2 (b), TiAl45-8 (c), and TiAl46-8 (d) after oxidation in 50 mL/min air flow at 850 and 950 °C for 10 h

8 and TiAl46-8 were more stable. It can be observed in Fig. 3(a) small variations, and in particular notable difference in the 2-6 h range between both high Nb-containing alloys though it is attributed to the calculation of the power exponent. The mass gain being very low (Fig. 2a), artifacts from the measure itself by TGA is likely responsible. It is reasonable to conclude that during the 10-h isothermal oxidation in air at 850 °C, the power exponents x (Eq 1) for the high Nb-containing alloys TiAl45-8 and TiAl46-8 were rather constant and described a quadratic growth ($x \sim 2$). This suggested that the higher content of Nb promoted the formation of protective oxides (alumina) and reduces the formation of detrimental rutile.

Different observations derive from the values of the power exponents x (Eq 1) at 950 °C (Fig. 3b). In both cases of low and high Nb-containing alloys, the power exponents x increased suggesting that a rather protective oxides scale was formed onto the samples surface. However, it is clear from Fig. 3(b) that the kinetic power exponent x (Eq 1) increases faster in the case of the high Nb-containing alloys TiAl45-8 and TiAl46-8. Initially, the oxidation kinetics were similar for all low and high Nb-containing alloys but quickly over 2 h at 950 °C, the beneficial effect of Nb addition is observed. Considering the lower weight gain (Fig. 2b) and the higher values of the power exponents (Fig. 3b), it can be concluded that high Nb content reduces the formation of titanium oxide and promotes the formation of a more protective oxides scale.

3.3 Phase Analysis of the Oxides Scale

The nature of the oxides scales were studied by x-ray diffraction. The measures were realized on the surface, directly on the oxide layer. When significant spallation occurred (TiAl45-2 and TiAl48-2 after 10 h at 950 °C), the XRD patterns were realized anyway on the samples' surface. Figure 4 displays the results. The XRD patterns of the original materials are shown in Fig. 4. The patterns realized after 10 h oxidation at both 850 and 950 °C for TiAl45-2, TiAl48-2, TiAl45-8, and TiAl46-8 are shown in Fig. 4(a)-(d), respectively.

In Fig. 4, the XRD patterns of the original materials as processed are very similar. All four alloys exhibited clearly the γ-TiAl phase (γ) as main constituent. A low amount of the α-Ti_3Al phase (α) was also revealed. Moreover, the β-TiAl phase (β) was found for TiAl45-8 and TiAl46-8 (Fig. 4c and d) as a result of high Nb content (Ref 18, 19). The phases of the bulk material were not reported on the XRD patterns after oxidation at 850 and 950 °C in Fig. 4. Only the phases formed due to oxidation were highlighted for clarity.

After short oxidation, either at 850 or 950 °C, all the alloys exhibited the same phases on their surface. Four phases were identified as products of the oxidation tests (Fig. 4): two oxides: Corundum Alumina Al_2O_3 (♥) and Rutile TiO_2 (♦); and two nitrides: Titanium Nitride TiN (■) and Aluminum Titanium Nitride Ti_2AlN (♠). The formation of nitrides, and in particular titanium nitride, was found detrimental for the oxidation resistance of γ-TiAl alloys (Ref 1, 3, 5, 7). Nitride

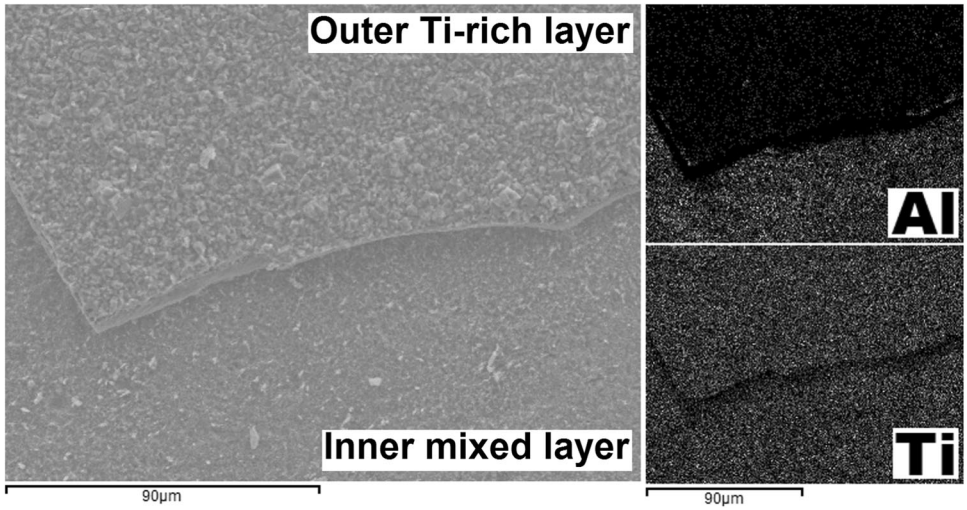

Fig. 5 Outer layer and underlying consistent layer on a $10 \times 10 \times 10$ mm^3 Ti-48Al-2Cr-2Nb specimen oxidized in static air at 850 °C for 100 h

formation impedes the growth of a continuous Al_2O_3 barrier layer in the inner part of the oxide scale. However, Becker et al. (Ref 10) drew the opposite conclusion suggesting that the formation of titanium nitride decreases the activity of Ti and increases that of Al, thus promoting the formation of Al_2O_3. From the XRD patterns in Fig. 4, it was hard to draw conclusions about the formation of nitrides. The intensity of the peaks relative to nitrides (■ and ♠ in Fig. 4) was very low in all cases. In addition, nitrides form in the inner part of the oxides' scale in the vicinity of the scale-substrate interface (Ref 10, 12). Therefore, the intensity of the XRD peaks relative to nitrides depends significantly on the oxides' scale thickness. When compared to the main phase of the bulk material (γ in Fig. 4), it is suggested a lower amount of nitrides when the Nb content was higher although further investigation are necessary.

After only 10 h at 850 °C in 50 mL/min air flow, the XRD patterns of TiAl45-2 (Fig. 4a) and TiAl48-2 (Fig. 4b) exhibited peaks relative to the oxides of high intensity. The main phase identified remained γ-TiAl (γ) from the underlying bulk material but a significant amount of rutile TiO_2 (♦) was found. On the other hand, the XRD patterns of TiAl45-8 (Fig. 4c) and TiAl46-8 (Fig. 4d) exhibited peaks relative to oxides of much lower intensity, in particular TiO_2 (♦). The γ-TiAl (γ) phase from the bulk materials was clearly the main phase identified. This is consistent with the results from thermogravimetry in Fig. 2 which clearly suggest a more severe oxidation of the low Nb-containing alloys. However, there was no evidence of a major growth of protective alumina Al_2O_3 for high Nb-containing alloys (Fig. 4c and d). As it was mentioned previously, there is competitive oxidation of Ti and Al in γ-TiAl alloys (Ref 1-8). Although further investigation is necessary, it is suggested that the higher amount of Nb in TiAl45-8 and TiAl46-8 reduced the formation of detrimental rutile TiO_2. This is consistent with previous observations suggesting that Nb lowers the activity of Ti and reduces oxygen vacancies (Ref 2, 4, 10).

After 10 h at 950 °C, TiAl45-2 and TiAl48-2 exhibited substantial spallation. Therefore, the reader must be aware that the XRD patterns in Fig. 4(a) and (b) do not take into consideration a significant amount of spalled oxide. Despite serious spallation, the low Nb-containing alloys and in particular TiAl45-2 exhibited high intensity peaks of rutile TiO_2 (♦). Peaks from the bulk material were very low for TiAl45-2 in Fig. 4(a). Instead, the intensities of the bulk materials' peaks of the high Nb-containing alloys TiAl45-8 and TiAl46-8 were relatively high (γ and α in Fig. 4c and d) although rutile (♦) was found in a large amount. It is interesting to note that the XRD patterns of the high Nb-containing alloys in Fig. 4(c) and (d) exhibit peaks relative to the rutile (110) plane ($2\theta \sim 27.5°$) of the highest intensity. This suggested that the outermost portion of the oxides scale was rich in TiO_2 grown by outward cation diffusion in that direction. On the contrary, both low Nb-containing alloys in Fig. 4(a) and (b), of which a substantial amount of oxides scale had spalled, exhibited peaks relative to the (110) plane of much lower intensity. It suggested that the nature of the outer scale, and thus the spalled oxide when spallation occurred, was TiO_2 preferentially oriented in the [110] direction.

It has been widely reported that the outer layer of the oxides scale of γ-TiAl alloys consisted for the most part of titanium oxide (Ref 1, 3-8, 10, 12, 14). In Fig. 5, a SEM micrograph shows a spalled area where the outer layer and the underlying consistent layer can be observed on top and at the bottom of the image, respectively. The spallation occurred after oxidation for 100 h in static air at 850 °C and subsequent air cooling (Ref 18). In Fig. 5, the element distribution maps measured by EDS for Al (top right) and Ti (bottom right) were inserted. Elements are represented by white dots as a result of EDS element mapping.

It is clear from the element distribution maps in Fig. 5 that the outer layer was rich in Ti and very poor in Al, indicating that the outer layer prone to spallation was mainly composed by TiO_2. On the other hand, the underlying oxides layer which remained consistent to the specimen contained a significant amount of Ti and Al, suggesting that the underlying layer is a mixed $TiO_2 + Al_2O_3$ layer. The outermost oxide scale of high Nb-containing alloys was a mixture of $TiO_2 + Al_2O_3$, similar to the underlying layer at the bottom of Fig. 5. This observation was confirmed by close examination of the oxide morphologies. The outer layer in Fig. 5 exhibited coarse oxide particles typical of TiO_2. On the other hand, the underlying or inner layer was composed by smaller oxide crystals showing different

shape: granular crystals typical of TiO_2 and needle-like crystals typical of Al_2O_3. This observation was consistent to previous research (Ref 5, 10, 12, 14). This confirms that addition of Nb slows down the formation of rutile TiO_2, which explains the lower mass gain due to oxidation and better resistance to spallation of high Nb-containing alloys.

4. Conclusion

The oxidation behavior in air of low and high Nb-containing γ-TiAl alloys was studied. Four alloys with different content of Al and Nb were produced by electron beam melting: TiAl45-2, TiAl48-2, TiAl45-8, and TiAl46-8. The following conclusions could be drawn:

- Oxidation up to 750 °C was negligible for all four materials.
- During constant heating at low rate (0.5 °C/min), low Nb-containing alloys clearly exhibited more severe oxidation than high Nb-containing alloys above 850 °C (Fig. 1).
- The mass gain due to isothermal oxidation at 850 °C for only 10 h of the low Nb-containing alloys was at least twice that of the high Nb-containing alloys (Fig. 2a). The analysis of the oxidation kinetics suggested that both high Nb-containing alloys followed a parabolic law over the 10 h isothermal oxidation at 850 °C. On the other hand, the kinetics law at 850 °C for the low Nb-containing alloys evolved from initially linear to eventually cubic.
- The mass gain due to isothermal oxidation at 950 °C for only 10 h of the low Nb-containing alloys was as well at least twice that of the high Nb-containing alloys (Fig. 2b). Regarding the kinetics of oxidation, it appeared that the oxides scale formed on high Nb-containing alloys was more protective than that grown on the low Nb-containing alloys.
- All four alloys TiAl45-2, TiAl48-2, TiAl45-8, and TiAl46-8 exhibited oxides of the same nature (Fig. 4). There was no evidence of suppression of rutile TiO_2 growth by Nb addition or promotion of alumina Al_2O_3 formation. Instead, Nb addition in this range seems to slow down the formation of rutile which is fast growing and subject to spallation.

Acknowledgment

The authors acknowledge the support of Arcam AB and AvioProp for the production by Electron Beam Melting of the studied materials.

References

1. M. Schutze, M. Hald, C. Lang, S. Melsheimer, and A. Rahmel, Intermetallic Disilicides and Titanium Aluminides—A New Class of Structural High Temperature Materials Under the Aspect of Their High Temperature Oxidation Resistance, *Pure Appl. Chem.*, 1997, **69**(11), p 2335–2341
2. M. Yoshihara and K. Miura, Effects of Nb Addition on Oxidation Behavior of TiAl, *Intermetallics*, 1995, **3**, p 357–363
3. S. Taniguchi and T. Shibita, Influence of Additional Elements on the Oxidation Behaviour of TiAl, *Intermetallics*, 1996, **4**, p S85–S93
4. J.P. Lin, L.L. Zhao, G.Y. Li, L.Q. Zhang, X.P. Song, F. Ye, and G.L. Chen, Effect of High Nb on Oxidation Behavior of High Nb Containing TiAl Alloys, *Intermetallics*, 2011, **19**, p 131–136
5. V.A.C. Haanappel, H. Clemens, and M.F. Stroosnijder, The High Temperature Oxidation Behaviour of High and Low Alloyed TiAl-Based Intermetallics, *Intermetallics*, 2002, **10**, p 293–305
6. G. Chen, Z. Sun, and X. Zhou, Oxidation and Mechanical Behavior of Intermetallic Alloys in the Ti-Nb-Al Ternary System, *Mater. Sci. Eng.*, 1992, **A153**, p 597–601
7. M. Mitoraj, E. Godlewska, O. Heintz, N. Geoffroy, S. Fontana, and S. Chevalier, Scale Composition and Oxidation Mechanism of the Ti-48Al-8Nb Alloy in Air at 700 and 800 °C, *Intermetallics*, 2011, **19**, p 39–47
8. Y. Shen, X. Ding, and F. Wang, High Temperature Oxidation Behavior of Ti-Al-Nb Ternary Alloys, *J. Mater. Sci.*, 2004, **39**, p 6583–6589
9. K. Kothari, R. Radhakrishnan, and N.M. Wereley, Advances in Gamma Titanium Aluminides and Their Manufacturing Techniques, *Prog. Aerosp. Sci.*, 2012, **55**, p 1–16
10. S. Becker, A. Rahmel, M. Schorr, and M. Schütze, Mechanism of Isothermal Oxidation of the Intermetallic TiAl and TiAl Alloys, *Oxid. Met.*, 1992, **38**, p 425–464
11. T. Tetsui, Effects of High Niobium Addition on the Mechanical Properties and High Temperature Deformability of Gamma TiAl Alloys, *Intermetallics*, 2002, **10**, p 239–245
12. V.A.C. Haanappel and M.H. Stroosnijder, The Effect of Ion Implantation on the Oxidation Behavior of TiAl-Based Intermetallic Alloys at 900 °C, *Surf. Coat. Technol.*, 1998, **105**, p 147–154
13. G. Schumacher, F. Dettenwanger, M. Schutze, U. Hornauer, E. Richter, E. Wieser, and W. Moller, Microalloying Effects in the Oxidation of TiAl Materials, *Intermetallics*, 1999, **7**, p 1113–1120
14. D. Pilone and F. Felli, Isothermal Oxidation Behavior of TiAl-Cr-Nb-B Alloys Produced by Induction Melting, *Intermetallics*, 2012, **26**, p 36–39
15. R. Pflumm, A. Donchev, S. Mayer, and H. Clemens, High-Temperature Oxidation Behavior of Multi-Phase Mo-Containing γ-TiAl-Based Alloys, *Intermetallics*, 2014, **53**, p 45–55
16. S.W. Kim, J.K. Hong, Y.S. Na, J.T. Yeom, and S.E. Kim, Development of TiAl Alloys with Excellent Mechanical Properties and Oxidation Resistance, *Mater. Des.*, 2014, **54**, p 814–819
17. M. Terner, S. Biamino, P. Epicoco, A. Penna, O. Hedin, S. Sabbadini, P. Fino, M. Pavese, U. Ackelid, P. Gennaro, F. Pelissero, and C. Badini, Electron Beam Melting of High Niobium Containing TiAl Alloy: Feasibility Investigation, *Steel Res. Int.*, 2012, **83**(10), p 943–949
18. M. Terner, S. Biamino, F. Pelissero, S. Sabbadini, P. Fino, M. Pavese, and C. Badini, Oxidation Behavior of Ti-47Al-2Cr-2Nb and Ti-45Al-2Cr-8Nb Produced by Electron Beam Melting, *Proc. Euro PM*, 2013, **2**, p 55–60
19. G.L. Chen, X.J. Xu, Z.K. Teng, Y.L. Wang, and J.P. Lin, Microsegregation in High Nb Containing TiAl Alloy Ingots Beyond Laboratory Scale, *Intermetallics*, 2007, **15**, p 625–631